Stabilisation of distearoylphosphatidylcholine lamellar phases in propylene glycol using cholesterol

Journal:	*Molecular Pharmaceutics*
Manuscript ID:	mp-2013-00140u.R1
Manuscript Type:	Article
Date Submitted by the Author:	02-Aug-2013
Complete List of Authors:	Harvey, Richard; King's College London, Institute of Pharmaceutical Science Ara, Nargis; King's College London, Institute of Pharmaceutical Science Heenan, Richard K.; Rutherford Appleton Laboratory (Chilton, UK), Barlow, David; King's College London, Institute of Pharmaceutical Science Quinn, Peter; King's College London, Institute of Pharmaceutical Science Lawrence, M Jayne; King's College London, Institute of Pharmaceutical Science

Stabilisation of distearoylphosphatidylcholine lamellar phases in propylene glycol using cholesterol

Richard D. Harvey[*‡□], *Nargis Ara*[□], *Richard K. Heenan*[§], *David J. Barlow*[□], *Peter J. Quinn*[‡□] *and M. Jayne Lawrence*[‡□]

[□]Pharmaceutical Biophysics Group, Institute of Pharmaceutical Science, King's College London, 150 Stamford Street, London SE1 9NH, UK.

[§]ISIS Facility, Rutherford Appleton Laboratory, Chilton, Oxon OX11 0QX, UK.

KEYWORDS: propylene glycol-liposomes, X-ray diffraction, small-angle neutron scattering, drug delivery.

ABSTRACT

Phospholipid vesicles (liposomes) formed in pharmaceutically acceptable non-aqueous polar solvents such as propylene glycol are of interest in drug delivery because of their ability to improve the bioavailability of drugs with poor aqueous solubility. We have demonstrated a stabilising effect of cholesterol on lamellar phases formed by dispersion of distearoylphosphatidylcholine in water/propylene glycol solutions with glycol concentrations ranging from 0 to 100%. The stability of the dispersions was assessed by determining the effect of propylene glycol concentration on structural parameters of the lamellar phases using a complimentary combination of X-ray and neutron scattering techniques at 25°C and in the case of X-ray scattering at 65°C. Significantly although stable lamellar phases (and liposomes) were formed in all propylene glycol solutions at 25°C, the association of the glycol with the liposomes' lamellar structures, led to the formation of interdigitated phases, which were not thermostable at 65°C. With the addition of equimolar quantities of cholesterol to the dispersions of distearoylphosphatidylcholine, stable lamellar dispersions (and indeed liposomes) were formed in all propylene glycol solutions at 25°C, with significant lateral phase separation of the bilayer components only detectable in propylene glycol concentrations above 60% w/w. We propose that the stability of lamellar phases of the cholesterol-containing liposomes formed in propylene glycol concentrations of up to 60% w/w represent potentially very valuable drug delivery vehicles for a variety of routes of administration.

INTRODUCTION

The ability of the phospholipid, dipalmitoylphosphatidylcholine, to form liposomes in the non-aqueous polar solvents, ethylene glycol and glycerol[1] has encouraged the study of liposomes in mixtures of water and the pharmaceutically acceptable co-solvent, propylene glycol (PG).[2-4] Such vesicles have considerable potential for a variety of drug delivery applications as there are a number of significant advantages to be gained from their use. Their main advantage is arguably the increase in bioavailability of poorly-water soluble drugs achieved by encapsulating them into propylene glycol containing liposomes[5, 6] resulting from the almost exponential increase in solubility of poorly-water soluble drugs that frequently occurs upon increasing propylene glycol concentration. In addition to improving drug loading into the liposomes, the presence of propylene glycol in the formulation enhances the chemical stability of the encapsulated drug by protecting it from oxidation or hydrolysis.[7] In the case of drugs formulated for topical delivery the use of propylene glycol further augments the dermal penetration of liposomes specifically designed to enhance skin delivery.[8] Moreover the presence of propylene glycol may result in the production of smaller vesicles.[4] Advantages in terms of liposome stability may also be gained due to the increase in the viscosity of the dispersion.

Most work to date has examined the preparation of liposomes in mixtures containing 10-20% w/w propylene glycol.[6, 9, 10] Indeed very few studies have reported on liposome formation in mixtures containing higher amounts of propylene glycol, e.g. Jeong and Oh[11] used 50% w/w propylene glycol while our own studies[3] were the first to examine liposome formation in propylene glycol concentrations up to 100%. Furthermore, Jeong and co-workers [7, 11] established the formation of lamellae in pure propylene glycol mixtures but they did not establish the existence of liposomes.

The utility of liposomal formulations containing both lipids and propylene glycol depends on the type of lipids used and the concentration of PG. Most of the studies reported demonstrate that PG much interact with the lipid bilayers in some way because it destabilises their lamellar structure, promoting the formation of an isotropic phase at temperatures above the gel to liquid phase transition.[12] In the case of the phosphatidylcholines (PC) commonly used to form liposomes, use of fully-saturated lipids allows higher concentrations of PG to be incorporated which in turn further augments drug loading.[6] Recently, cholesterol has been added to PC based liposome formulations prepared using less than 20% w/w propylene glycol.[9, 10] Although it might be anticipated that the presence of cholesterol should enhance vesicle stability in propylene glycol solutions allowing them to support higher concentrations of non-aqueous solvent, there is no evidence to support this hypothesis. It is clear that the ability to increase the propylene glycol concentration in such vesicles would increase the range of drugs able to be solubilised and thus extend the potential range of PG-liposome use. To date there have been no systematic studies performed examining in detail the physicochemical properties of liposomes formed in water/propylene glycol mixtures.

In this study we build on our earlier study[3] to assess the stability at the molecular level of distearoylphosphatidylcholine lamellar phases in response to increasing concentrations of propylene glycol co-solvent, in the presence and absence of equimolar quantities of cholesterol, in order to try to establish the maximum concentration of propylene glycol which may be used in PG-liposome manufacture. The investigations were performed using a combination of small-angle synchrotron X-ray (SAXS) and neutron scattering (SANS) techniques with samples prepared for the former with an equal mass of lipid and propylene glycol solutions and for the latter in excess bulk solvent, to encourage the formation of liposomal structures. Additionally freeze-fracture electron microscopy was used to establish the formation of liposomes. Lamellar (bilayer) stability as a function of temperature was determined using SAXS. The results of the scattering studies provide corroborative and complimentary evidence for the influence of propylene glycol on bilayer stability, and enable us to proffer an explanation for the stabilising effect of cholesterol.

EXPERIMENTAL SECTION

Materials. The lipids 1,2-distearoyl-*sn*-glycero-3-phosphocholine (DSPC), 1,2-distearoyl(d_{70})-*sn*-glycero-3-phosphocholine (d-DSPC) and cholesterol were all purchased from Avanti Polar Lipids (USA). Spectroscopic grade chloroform was obtained from Fluka (UK). Propylene glycol (1,2-propanediol or h-PG) was supplied by Sigma-Aldrich (UK) and 1,2-propanediol-d_8 (d-PG) was obtained from QMX Laboratories (UK). Deuterium oxide (99.9 %) was supplied from Aldrich (UK). All materials were of the highest grade possible and were used as received. Double-distilled water from a well-seasoned all-glass still was used throughout the study.

Synchrotron X-ray Scattering Sample Preparation. Samples for X-ray diffraction examination were prepared by dissolving DSPC or an equimolar mixture of DSPC and cholesterol in chloroform/methanol (2:1, v/v) before removal of the organic solvent by evaporation under a stream of oxygen-free dry nitrogen at 45°C and storage under high vacuum for two days at 20°C. The lipids were subsequently solvated with an equal weight of water, h-PG or mixtures of the following designated proportions of PG and water, namely 0, 20, 40, 60, 80, 90 and 100% w/w h-PG (respectively 0, 5.6, 13.6, 26.2, 48.6, 68.1 and 100 mol% glycol). The resulting lipid suspensions were stirred thoroughly with a thin needle, sealed under argon, and annealed by thermally cycling between 20 and 65°C 20 times to ensure a complete mixing and solvation of the lipids. The samples were stored under argon at a temperature above 4°C. Prior to careful stirring and transfer into the X-ray diffraction measurement cell, the lipid dispersions were equilibrated for 5 hours at 25°C.

X-ray Scattering Measurements and Data Analysis. The X-ray scattering intensity data from dispersions of DSPC and DSPC/cholesterol in aqueous solutions of PG were recorded on Beamline 16.1 of the Daresbury Synchrotron Radiation Source (Warrington, UK). The lipid dispersions were sandwiched in a copper cell of 1 mm thickness between two mica windows and mounted on a cryostage (Linkam Scientific Instruments Ltd., UK) and equilibrated for 2 min in the sample cell at the desired temperature (25°C and 65°C after heating at a rate of at 5°C per min) before recording the scattering accumulated over 2 min. The X-ray wavelength was 0.141 nm and focused to a beam of dimensions 0.2 mm vertical × 2.5 mm horizontal in a configuration that minimizes parallax error.[13] The small-angle X-ray scattering (SAXS, $2\Theta = 0.043° – 7.9°$) was recorded using a quadrant multiwire delay-line detector. The detector was calibrated using the *d*-spacings of wet rat-tail collagen[14] with a sample to SAXS detector distance of 1.5 m. The wide-angle X-ray scattering (WAXS) was collected using an INEL detector[15] which was calibrated using the *d*-spacings of high-density polyethylene [16]. The setup, calibration and facilities available on Station 16.1 are described elsewhere.[17] After correction of the raw data by subtraction of the background scattering from both solvent and sample cell the Bragg peaks were fitted to Voigt-area functions using PeakFit software (v4.12; Systat Software Inc.) as described elsewhere.[18]

To obtain estimates of bilayer thickness (d_m) the distance between peaks of highest relative electron density, taken to represent the phosphate residues on either side of the phospholipid bilayer, and the thickness of the intervening solvent layer (d_s) between successive bilayers, the electron density profiles of the lamellar structures were calculated. The dimensions of the solvent layer (d_s) are obtained by subtracting d_m from the lamellar repeat spacing (d). It is recognized that this does not represent the true dimension of the solvent layer in the unit cell because the lipid head groups extend 4-5 Å into this region so the true space is of the order of 8-10 Å less than the calculated value.[19] Nevertheless, it is reasonable to assume that this lipid component of the electron density profile is similar for the different lipid mixtures so that differences in d_s should reflect differences in solvation of the bilayers.

The relative electron densities were derived from the following equation:[20, 21]

$$\rho(x) = (\frac{2}{d}) \cdot \sum g(h) \cdot \left|F(h)\right| \cdot \cos(2\pi x h / d) \qquad (1)$$

where x is the distance from the centre of the bilayer, d the lamellar repeat period, $g(h)$ the phase for the h^{th} order, and the summation is over diffraction orders h, $F(h)$ is the structure amplitude. For the unoriented X-ray diffraction pattern the absolute value of the structure amplitude was set equal to $\{h^2 I(h)\}^{1/2}$. [20]

Four peaks of X-ray scattering intensity ($I(h)$) representing the first four-orders of a lamellar phase of each sample were used to calculate the Fourier reconstruction of electron intensity. The phase g(h) can only be 1 or -1 by assuming a centrosymmetric structure in the multibilayer stack structure. Electron density calculations were performed for all combinations of phase angles but the only combination fitting a centrosymmetric diffraction profile expected of a multibilayer structure was –, –, +, – for all the diffraction profiles examined. This phase combination has been reported consistently for the saturated phosphatidylcholines in the gel phase: [22] the peak-to-peak distance between the electron dense region on either side of the bilayer, d_m, represents the bilayer thickness and water thickness (d_s) is represented by the distance between peaks of electron density in adjacent bilayers.

Vesicle Preparation for Small Angle Neutron Scattering Studies. Lipid films were formed in 20 mL glass vials by evaporation of solvent from chloroform/lipid solutions containing 2 mgmL^{-1} total lipid, on a Buchi 111 rotary evaporator (Buchi Labortechnik AG, Switzerland). The resultant dry lipid films were solvated in 2 g of the appropriate solvent. Hydrogenated lipids, with and without an equimolar quantity of hydrogenated cholesterol, were solvated with either pure D_2O, or d_8-PG, or mixtures of these two solvents containing 20, 40, 60 and 80% w/w d_8-PG (5.6, 13.7, 26.3, and 48.8 mol% glycol respectively) to give a final lipid concentration of 0.1% w/w. Corresponding samples containing chain-deuterated d_{70}-DSPC (with or without hydrogenated cholesterol) were prepared in h-PG-H_2O mixtures of 0, 20, 40, 60, 80 and 100% w/w PG (respectively 0, 5.6, 13.6, 26.2, 48.6 and 100 mol% glycol). In all cases, solvation was achieved by initially incubating the lipid film in the relevant solvent at 65°C for 30 minutes, followed by vortex mixing and by bath sonication (Fischerbrand FB11203) for 10 minutes. For the samples up to and including 60% w/w d_8- or h-PG, the solvated lipid dispersions were extruded (Avanti Mini-Extruder) by three passages through 0.1 µm polycarbonate membrane filters (Whatman, Nuclepore), and were allowed to anneal at room temperature for 1 hr. Samples containing 80 and 100% glycol were too viscous to be readily extruded through the polycarbonate membrane and were therefore bath sonicated for ~30 min to form uniform dispersions.

SANS Measurements and Data Analysis. SANS measurements were performed using a 12 mm diameter neutron beam on the LOQ beam line at the ISIS pulsed neutron source (ISIS, STFC Rutherford-Appleton Laboratory, Didcot, UK). LOQ uses pulses of neutrons of wavelengths between 2.2 Å and 10 Å which are separated by time-of-flight and detected by a 64 cm × 64 cm, two dimensional detector at a fixed distance of 4.1 m from the sample. Wavelength-dependent corrections were made to allow for the incident spectrum, detector efficiencies and measured sample transmissions in order to create a composite SANS pattern (as described in detail in

Heenan *et al* [23]). This gives a scattering vector Q = (4π/λ)sin(θ/2) in the range of Q = 0.008 to 0.22 $Å^{-1}$. Comparisons with scattering from a partially deuterated polystyrene standard allowed absolute scattering cross sections to be determined with an error of ± 2.0%. For the purposes of comparison with the SAXS data, SANS scattering curves were plotted as S (1/*d*) versus intensity instead of Q (2π/*d*) versus intensity.

Dispersions of either 1 mg/g total lipid DPSC or DSPC/cholesterol (an appropriate dilution to avoid inter-particulate interactions) were placed in scrupulously cleaned disc-shaped fused silica cells with either a 1 or 2 mm path length, depending upon whether the solvent was hydrogenated or deuterated, respectively. Measurements were made at 25 ± 0.1°C. Backgrounds of the appropriate solvent were subtracted. All fitting procedures included flat background corrections to allow for any mismatch in the incoherent and inelastic scattering between the sample and solvents. Fitted background levels were always checked to ensure that they were of a physically reasonable magnitude.

The combination of the size of the vesicles coupled with the Q range employed in the SANS measurements reported here, meant that the vesicles could be treated (to a good first approximation) as randomly oriented infinite planar sheets of thickness τ, for which the scattering is described as:

$$P(Q) = 2\pi(\Delta\rho)^2 S\tau^2 \frac{1}{Q^2}\frac{\sin^2(Q\tau/2)}{(Q\tau/2)^2} \qquad (2)$$

where ($\Delta\rho$) is the neutron scattering length density difference between sheet and solvent and *S* is the area of sheet per unit sample volume. Kotlarchyk and Ritzau [24], following the work of

Shibayama and Hashimoto,[25] integrated equation (2) for the case where the sheet thickness is polydisperse. Since the scattering is significant only in a direction normal to the sheet, it is possible to convolute with a Gaussian to model diffuse sheet boundaries. In this case, the $1/Q^2$ second term in (1) is a Lorentz factor $L_N(Q)$ which allows for random orientation of the planar sheets. To allow for deviations from a perfectly flat sheet, the Lorentz factor can be modified,[26] to allow for a Gaussian distribution of surface normals σ, around the Q vector coupled to a lateral extent $2R$ of the sheet:

$$L_N(Q) = \frac{1}{1 + \frac{1}{2} Q^2 (R\sigma)^2} \qquad (3)$$

For the case of multilamellar vesicles, the vesicle lamellae were treated as a one-dimensional paracrystalline stack, with the scattering from individual layers modelled as described above, and successive plane spacings chosen at random from a Gaussian distribution. The structure factor for the paracrystal is calculated according to Kotlarchyk and Ritzau,[24] with parameters: M, the number of layers in the stack; d, their mean separation; and $\sigma(d)/d$, the width of the Gaussian distribution in the plane positions. Number of layers M is generally here only approximately determined, it particularly controls the upturn in scattering at small Q where the total thickness of the stack is seen; infinitely thick stacks would have just a Bragg peak on a nearly flat background.

In modelling the SANS data for systems involving only unilamellar vesicles, the vesicle lamellae were treated as sheets of uniform scattering length density, with a mean thickness d_m, a Schultz polydispersity characterised by $\sigma(d_m)/d_m$, and local extent characterised by $R\sigma$ in equation (2). The fits to the SANS data were thus obtained by least-squares refinement of the four parameters, d_m, $\sigma(d_m)/d_m$, $R\sigma$ and the absolute scale factor.

For those systems considered to involve a mixed population of unilamellar and multilamellar vesicles, the SANS data were modelled assuming (isolated) infinite planar sheets as well as one-dimensional paracrystals of these (with d_m, $\sigma(d_m)/d_m$ and $R\sigma$ constrained to be the same for the isolated and stacked lamellae, a not unreasonable assumption). Here, therefore, the fits to the SANS data were obtained by least-squares refinement of the eight parameters, d_m, $\sigma(d_m)/d_m$, $R\sigma$, M, d, $\sigma(d)/d$ and the absolute scale factors for the unilamellar and multilamellar vesicles.

In all cases the least-squares refinements were performed using the model-fitting routines provided in the FISH software.[27]

Freeze-Fracture Electron Microscopy. Lipid dispersions composed of equimolar quantities of DSPC/cholesterol were prepared in 20%, 60% w/w and 100% propylene glycol at a total lipid concentration of 5 mg/ml, by 5 minutes sonication using a Lucas Dawe probe sonicator fitted with a tapered micro tip (operating at 15% of its maximum output). Small aliquots (~10 μL) of freshly prepared lipid dispersions were flash frozen at 77 K using liquid nitrogen and then fractured under vacuum (2×10^{-4} Pa). These preparations were shadowed using platinum/carbon at 318 K and then carbon blacked at 100°C under vacuum. The cleaned replicates were mounted on Formvar® (polyvinyl formal) and carbon coated copper grids and viewed using a transmission electron microscope (Philips EM 301G) operating with an accelerating voltage of 80 kV.

RESULTS

X-ray Scattering from Dispersions of DSPC. DSPC is able to form lamellar phases at 25°C in all of the PG/water mixtures, even at concentrations of up to 100% PG, as shown in the X-ray scattering intensity profiles in Figure 1A which clearly show the regular spacing of Bragg reflections indexing at least three orders of a lamellar structure for each of the solvent mixtures investigated. All of the PG-containing samples show a marked shift in the position of the diffraction peaks from that obtained for DSPC in water to higher angles, indicating a decrease in repeat spacing induced by the presence of the glycol. Analysis of the electron density profiles (Fig. 3) reveals a decrease in *d*-spacing from 67.0 Å for DSPC in water, to 53.2 Å in 20% w/w PG (Fig. 3A & B). There is no significant change in *d*-spacing between 40 and 80% w/w PG (all ~56.0 Å) before a marked decrease is again observed at 90 and 100% w/w PG (both ~52.0 Å). Analysis of the calculated electron density profiles show that the bilayer separation for all of the DSPC samples remains roughly constant and unchanged from that observed in water, at ~19.0 Å (Fig. 6E). The most obvious effect of the addition of PG on DSPC bilayer structure is therefore a marked decrease in layer thickness (from 48.2 Å to 35.1 Å on addition of 20% w/w glycol) (Fig. 6C).

Comparison of the wide-angle scattering profiles for DSPC in water and 20% w/w PG (Fig. 1A) shows that the shoulder present in water on the higher-angle side of the gel phase peak centred at 0.23 $Å^{-1}$ is absent in the presence of this small amount of glycol. This observation suggests that while the chains remain in the gel phase, the tilt on the chains is abolished in the presence of propylene glycol.[28] In addition, the slight shift seen in the position of the WAXS peak from 0.23 to 0.24 $Å^{-1}$ in the presence of the glycol indicates a slightly tighter packing of the acyl chains (with a change in lateral chain spacing from ~4.35 Å to ~4.16 Å). The loss of chain tilt and concomitant decrease in bilayer thickness, are consistent with the formation of an interdigitated ($L_{\beta}I$) lamellar phase.[29] The appearance of a shoulder at S = 0.2 $Å^{-1}$ in the wide-angle region suggests a proportional increase in acyl chain disorder with increasing percentage of glycol in the solvent. This increasing disorder in the gel phase is most likely caused by the association of PG with the lipid headgroups or partitioning into the bilayers, which increases proportionately with PG concentration.[12]

Increasing the temperature above that of the phase transition for DSPC dispersions in water (T_c 54.0°C [30]) to 65°C causes a broadening of the first and second order diffraction peaks for glycol-containing samples with up to 60% w/w PG (Fig. 1B). This broadening of the first order diffraction peak and loss of higher order peaks indicates increasing disorder in the bilayers. Above 60% w/w PG, the lack of discernible scattering intensity suggests the formation of a reversible isotropic phase where the lipid becomes completely soluble in the PG/water mixture a result agreement with observations made by others.[12]

X-ray Scattering from Dispersions of DSPC and Cholesterol. The incorporation of 50 mol% cholesterol produces a marked difference in the response of the lipid dispersions at 25°C to increasing PG concentration in the bulk solvent. Some phase separation between the lipid and the sterol is evident in all of the samples, from 0 to 60% w/w PG (Fig. 2A), by the presence of the diffraction peak for crystalline cholesterol monohydrate at ~35.4 Å.[31] The repeat spacings for the DSPC/cholesterol lamellar phase show some fluctuation as the concentration of PG increases from 0 to 80% w/w (Fig. 6B), but the overall trend shows a slight increase in *d*-spacing from 75.1 Å in water to 77.4 Å. Because of the lack of higher order diffraction peaks discernible in the scattering profiles of samples with >40% w/w PG, electron density profiles could not be determined above this concentration of glycol. However, it is clear from layer thicknesses calculated from the phosphate-to-phosphate distances in the electron density profiles, which remain fairly constant at ~50 Å (Fig. 6D) that there is no evidence for the formation of an interdigitated phase. An interesting phase transition occurs above 90% w/w PG, with the appearance of a number of separate lamellar phases clearly present in 100% PG (Fig. 2A).

The data from the first order peaks of the diffraction profile for DSPC/cholesterol in 100% PG at 25°C can be fitted as four lamellar structures with *d*-spacings of 77.4, 64.1, 62.3 and 52.2 Å (Fig. 2A). The (001) and (002) reflections from phase separated cholesterol monohydrate crystals (at S = 0.028 $Å^{-1}$ and S = 0.059 $Å^{-1}$ respectively) are evident in the scattering profile. Some of the lamellar phase peaks can be directly related to those observed in other samples with lower PG concentrations. The lamellar structure at *d* = 77.4 Å surprisingly (because no water is present) coincides with that of DSPC/cholesterol in water, and the lamellar structure of *d* = 52.2 Å, which evolves with increasing % PG coincides with that observed for the interdigitated phase observed for pure DSPC in PG (Fig. 1A). The lamellar structures at *d*-spacings of 64.1 and 62.3 Å are not observed in PG less than 100% although cholesterol monohydrate can be seen in all the dispersions as equimolar amounts appear to be above the solubility limit of cholesterol in the DSPC under the conditions of the experiment.

At 65°C the phase separation between the DSPC and cholesterol is abolished for dispersions in water, 20% PG and 40% w/w PG (Fig. 2B). Both the first and second order diffraction peaks for these samples remain sharp up to 40% w/w PG, in contrast to the dispersion of DSPC in the corresponding water/PG solvent mixtures at the same temperature (Fig. 1B), implying that the sterol imparts a stabilising effect on the lamellar phase. The broadening of the peaks in the scattering profile for DSPC/cholesterol in 60% w/w PG, suggests the commencing of some structural disorder, in addition to the possible appearance of phase separated cholesterol. For

DSPC/cholesterol dispersions in 80% w/w PG and above, the elevated temperature leads to a loss of stability and the eventual formation of an isotropic phase in pure PG. It is interesting to note that from the SAXS intensity profiles obtained for both DSPC and DSPC/cholesterol dispersions in PG/water mixtures, the samples prepared in 60% w/w PG in each case retain their stability at 65°C.

Small Angle Neutron Scattering from Dispersions of DSPC. In contrast to the samples prepared for SAXS experiments which comprised lipid-rich dispersions in solvent, the SANS samples were prepared as vesicular dispersions of lipid in an excess of bulk solvent phase. The neutron scattering intensity profiles for samples of chain-deuterated DSPC prepared in the different PG-water mixtures, together with fitted curves obtained from modelling the data assuming mixtures of planar bilayer and paracrystalline stacks, are shown in Figure 4A. The same model was used to analyse the scattering profiles obtained from h-DSPC dispersed in mixtures of d_8-PG and D_2O (Fig. 4B). With the exception of d-DSPC solvated in pure PG, which could only be successfully modelled as a single planar infinite flat sheet[24] all other samples fitted the single and stacked bilayer model. In each case, the number of bilayers in the stacks was low at ~3, while the ratio of stack:single bilayer decreased with increasing PG concentration (from ~0.5 in 20% PG, to ~0.1 in 80% PG). The bilayer parameters of *d*-spacing, layer thickness and bilayer separation are summarised and compared with those determined by SAXS in Figures 6A, 6C and 6E. Reassuringly there is excellent agreement between the SANS and SAXS *d*-spacing data (fig. 6A), with similar trends to those described above for the SAXS data, in the effect of increasing PG concentration on bilayer thickness and separation (Figures 6C and 6E), with the 10 Å decrease in layer thickness of the interdigitated $L_{\beta}I$ phase also evident in the modelled SANS data.

Small Angle Neutron Scattering from Dispersions of DSPC and Cholesterol. Scattering curves for the two different contrasts of h-DSPC/h-cholesterol in deuterated solvents and d-DSPC/h-cholesterol in hydrogenated solvents are given together with their fitted model curves in Figures 5A and 5B. As with the modelled DSPC dispersions, all but the d-DSPC/cholesterol in pure PG (Figure 5B), could be modelled as mixtures of planar bilayers and paracrystalline stacks. At all PG concentrations for both contrasts, the mean number of layers in the stacks was again relatively low ~3 and the stack/single ratio remained at ~0.3 for all but the single-layer modelled 100% PG sample. In contrast to the fluctuating *d*-spacing determined by SAXS the modelled SANS data shows a more distinct trend for increasing repeat spacing, from ~72 Å to ~81 Å, with each incremental increase in PG concentration (Figure 6B). This swelling of the bilayer stacks seems not to be due to a change in the bilayer thickness, which remains fairly constant at ~48 Å in up to 60% w/w PG, before decreasing to ~43 Å at 80% w/w PG and ~40 Å in 100% PG (Figure 6D). The solvent layer data (Figure 6F) shows a clear increase in bilayer separation proportionally with increasing PG concentration.

The only discrepancy between the SAXS data and the systems modelled from the SANS data comes when we consider the results for DSPC/cholesterol dispersions in pure PG. Due to the nature of the single flat sheet model, for which the bilayer thickness parameter represents an average for the modelled system, the four separate lamellar phases resolved from the X-ray data are not apparent in the SANS data.

Freeze Fracture Electron Microscopy. The electron micrographs presented in Figure 7 represent probe-sonicated dispersions of DSPC/cholesterol in 20% w/w, 60% w/w and 100% PG, which were five times more concentrated than those prepared for SANS measurements, but about 100 times more dilute than those used for SAXS. Multi-lamellar and multi-vesicular vesicles (MLV and MVV) were clearly visible in the sample in 20% PG (Figure 7A). The lack of uniformity in size and morphology may be attributed to the manufacturing technique, which is notorious for producing polydisperse vesicle dispersions. A similar polydispersity of vesicle sizes was observed for DSPC/cholesterol in 60% w/ PG (Figure 7B), interestingly however, all of the vesicles appeared to be perfectly spherical in shape. The samples dispersed in pure propylene glycol (Figure 7C) showed vesicles of a highly polymorphic nature. Many of the vesicles appeared to have been frozen in the act of budding, a process thought to require localised domains of high membrane curvature,[32] which may result from the phase separation effects of membrane saturation with PG observed in the SAXS data.

DISCUSSION

The various effects of increasing PG concentration on the structure of and stability of DSPC and equimolar DSPC/cholesterol dispersions result from the quasi-amphiphilic nature of the PG and its ability to associate with the phospholipid bilayers.[12] The octonol/water partition coefficient (Log $P_{o/w}$) of propylene glycol is -1.35,[33] implying that it is approximately twenty times more soluble in water than it would be in a lipid bilayer. With all of the systems studied here under equilibrium conditions, therefore, the differences in the lipid volume fractions used to prepare samples for the SAXS and SANS experiments means that there will be proportionally less PG present in the vesicle bilayers used for neutron scattering, due to the large excess of bulk solvent, than in the dispersions used X-ray diffraction (for samples between 20 and 90% w/w PG). The relative effects of the PG solutions on the measured bilayer parameters, however, can nevertheless be compared for the samples used in both techniques.

The SAXS and SANS results from this study clearly show that lipid chain interdigitation occurs when DSPC is dispersed in PG/water mixtures. The molecular origins of this interdigitation cannot be determined directly from our data, but may be attributed to an increased headgroup solvation by the PG, partitioning of PG into the hydrophobic core of the bilayers, or to a combination of these two phenomena.[34] Although there is no direct evidence for the occurrence of either from the data, nevertheless some qualitative assumptions about the complex interplay between components in DSPC and DSPC/cholesterol dispersions in PG/water mixtures can be made.

For gel phase DPPC, partitioning of ethanol at concentrations of as little as 7% v/v (in water) induces the formation of an interdigitated $L_{\beta}I$ phase.[35] The increase in lipid molecular area required to induce such chain interdigitation is more than likely the result of solvent partitioning into the bilayer hydrophobic core, thus weakening the van der Waals interactions between the acyl chains themselves.[1, 29] The observed chain interdigitation for the DSPC-water-PG system could therefore be induced by a similar solvent partitioning. In the case of short-chain alcohol partitioning into phosphatidylcholine membranes, however, there is a concomitant swelling of the bilayers induced by a weakening of the van der Waals forces between the bilayers[34] and an increased flexibility (a lowering of the bending modulus k_c).[36] It is clear from the bilayer separations obtained in this study (fig. 6E) that swelling does not occur, as the interlamellar separations remain at ~20 Å, the limit of the steric overlap and protrusion forces which would prevent further approach between the lamellae.[37]

In addition to the putative effects of solvent penetration on increased molecular area and lipid chain interdigitation, PG partitioning may also decrease the gel-liquid phase transition temperature of the lipid acyl chains.[12] The wide angle data (fig. 1A), however, clearly show the existence of gel phase at all concentrations of PG at 25°C with significant fluid phase only present at 80% PG and above. It may well be, therefore, that the observed chain interdigitation is due in the main to an association of the glycol with the lipid headgroups, causing an increased molecular area.[34]

At 65°C, however, the significant penetration of PG into the DSPC bilayers at 80% glycol and above, is the most likely cause of the destabilisation of the bilayers,[12] which when coupled with a putative decrease in k_c above the lipid phase transition temperature,[38] facilitates disintegration of the lamellar structure and the formation of an isotropic phase.

The incorporation of an equimolar quantity of cholesterol along with DSPC in the water/PG mixtures has a significant effect on bilayer stability. Since bilayer thickness remains constant in up to 60% PG there is no apparent interdigitation, possibly resulting from the steric exclusion/impedance of solvent penetration into the interfacial region of the bilayers. Unlike with pure DSPC, the enhanced fluidising effect of 50 mol% cholesterol inclusion into DSPC bilayers[39] must significantly increase their flexibility as the lamellae swell proportionally with increasing % PG at 25°C. At 65°C there is evidence for lamellar phase present in up to 80% PG before the transition to isotropic phase above 90% PG (~50 and ~70 mol% PG respectively). Although this represents an increase in the stability of the lamellar phase over those of pure DSPC at the same temperature (where the transition to isotropic phase occurs above 80% PG), the stabilising effect appears to compete against the progressive phase separation of the cholesterol. The most dramatic manifestation of this effect is possibly that observed for DSPC/cholesterol in 100% PG at 25°C.

The relative stabilities of lipid lamellar phases in propylene glycol solutions have a number of implications, which may be applied to their use as drug delivery vehicles. In the main, vesicles used for drug delivery should exhibit long-term stability in order to increase their usefulness, in terms of their ease of manufacture and storage, and their ability to enhance the bioavailability of their drug payload upon administration. With respect to the vesicles formed from DSPC alone, their inherent instability when formed in various PG solutions, as evidenced by the formation of both interdigitated bilayers at low PG concentrations and isotropic phases above the main phase transition temperature,[12] might serve to limit their usefulness in drug delivery. However, such characteristics may prove useful for tuning PG-liposome properties in formulations for topical drug delivery, which could combine temperature sensitive drug release with the skin permeation enhancement facilitated by the propylene glycol.[7] It is clear that to broaden the scope of PG-liposomes beyond topical delivery formulations to include possible parenteral routes of administration,[6] the stability enhancement facilitated by the incorporation of cholesterol would be necessary. What the results of this study indicate is that equimolar DSPC/Cholesterol PG-liposomes are formed in up to 100% PG and would appear to be most stable at elevated temperatures in up to 60%w/w glycol. When one considers that to date most sterol-stabilised PG-liposomes have been formed in propylene glycol solutions of between 10 and 20%w/w,[6, 9, 10] the ability to form stable vesicle dispersions in higher concentrations of co-solvent would serve to further improve loading of drugs with poor aqueous solubility and increase the range of drugs which might benefit from incorporation into PG-liposomes.

FIGURES

Figure 1. Small-angle (left) and wide-angle (right) X-ray scattering intensity profiles recorded from dispersions of distearoylphosphatidylcholine in various aqueous propylene glycol solutions (%PG w/w) at A. 25°C and B. 65°C.

Figure 2. Small-angle (left) and wide-angle (right) X-ray scattering intensity profiles recorded from dispersions of equimolar mixtures of distearoylphosphatidylcholine and cholesterol in various aqueous propylene glycol solutions (%PG w/w) at A. 25°C and B. 65°C.

Figure 3. Representative electron density profiles calculated from small-angle X-ray scattering intensity profiles obtained at 25°C, of distearoylphosphatidylcholine dispersions in A. water and B. 20% w/w propylene glycol; dispersions of equimolar mixtures of distearoylphosphatidylcholine and cholesterol in C. water and D. 20% w/w propylene glycol.

Figure 4. Small-angle neutron scattering intensity profiles recorded at 25°C from dispersions of A. d_{70}-distearolyphosphatidylcholine in various hydrogenated aqueous solutions of propylene glycol (%PG w/w) and B. hydrogenated distearolyphosphatidylcholine in various deuterated aqueous solutions of propylene glycol (%PG w/w). The open circles show the experimental data and the solid lines show the fitted model. For some cases the error bars for these SANS scattering curves are very low and do not protrude beyond the symbols used to mark the points.

Figure 5. Small-angle neutron scattering intensity profiles recorded at 25°C from dispersions of equimolar mixtures of distearolyphosphatidylcholine and cholesterol containing A. d_{70}-distearolyphosphatidylcholine in various hydrogenated aqueous solutions of propylene glycol (%PG w/w) and B. hydrogenated distearolyphosphatidylcholine in various deuterated aqueous solutions of propylene glycol (%PG w/w). The open circles show the experimental data and the solid lines show the fitted model. In some cases the error bars for these SANS scattering curves are very low and do not protrude beyond the symbols used to mark the points.

Figure 6. Summaries of bilayer parameters obtained from measurements of DSPC (A,C & E) and DSPC/cholesterol (B, D & F) dispersions in propylene glycol solutions using both small-angle X-ray and small-angle neutron scattering techniques: A and B represent the lamellar repeat spacings (d), C and D represent the bilayer thicknesses (d_m) and E and F represent the solvent layer thicknesses (d_s).

Figure 7. Freeze-fracture electron micrographs of dispersions of equimolar mixtures of distearoylphosphatidylcholine and cholesterol in A. 20% w/w propylene glycol, B. 60% w/w propylene glycol and C. 100% w/w propylene glycol. In micrograph A, the arrow indicates the appearance of a lamellar stack. In each micrograph, the scale bar represents 200 nm.

AUTHOR INFORMATION

Corresponding Author

*Pharmaceutical Biophysics Group, Institute of Pharmaceutical Science, King's College London, 150 Stamford Street, London SE1 9NH, UK. E-mail: richard.d.harvey@kcl.ac.uk

Author Contributions

The manuscript was written through contributions of all authors. All authors have given approval to the final version of the manuscript. ‡These authors contributed equally.

ACKNOWLEDGMENT

The authors gratefully acknowledge Dr Tony Brain for his technical assistance with the freeze-fracture electron microscopy. We also thank the Science and Technology Facilities Council and the Rutherford Appleton Laboratory for the award of neutron beam time. King's College London is acknowledged for the award of a scholarship to NA.

SUPPORTING INFORMATION

Estimations for the Hamaker constant and interbilayer van der Waals forces for the multilamellar DSPC and DSPC/Chol dispersions in the PG/water mixtures described in this paper, are provided as supporting information. This information is available free of charge via the Internet at http://pubs.acs.org/.

ABBREVIATIONS

DSPC, distearoylphosphatidylcholine; Chol, cholesterol; PG, propylene glycol; SAXS, small-angle X-ray scattering; WAXS, wide-angle X-ray scattering; SANS, small-angle neutron scattering.

REFERENCES

1. McDaniel, R. V.; McIntosh, T. J.; Simon, S. A. Non-electrolyte substitution for water in phosphatidylcholine bilayers. *Biochim Biophys Acta* **1983,** *731*, 97-108.

2. Elsayed, M. M. A.; Abdallah, O. Y.; Naggar, V. F.; Khalafallah, N. M. PG-liposomes: novel lipid vesicles for skin delivery of drugs. *J Pharm Pharmacol* **2007**, 1447-1450.

3. Harvey, R. D.; Azad, N.; Quinn, P. J.; Lawrence, M. J. Effect of propylene glycol on bilayers formed by equimolar mixtures of phospholipid and cholesterol. *Eur Biophys J* **2005,** *34*, 698.

4. Kang, K. C.; Lee, C. I.; Pyo, H. B.; Jeong, N. H. Preparation and characterization of nano-liposomes using phosphatidylcholine. *J. Ind. Eng. Chem.* **2005,** *11*, 847-851.

5. Junyaprasert, V. B.; Singhsa, P.; Suksiriworapong, J.; Chantasart, D. Physicochemical properties and skin permeation of Span 60/Tween 60 niosomes of ellagic acid. *Int. J. Pharm.* **2012,** *423*, 303-311.

6. Yang, W.; Yu, X. C.; Chen, X. Y.; Zhang, L.; Lu, C. T.; Zhao, Y. Z. Pharmacokinetics and tissue distribution profile of icariin propylene glycol-liposome intraperitoneal injection in mice. *J Pharm Pharmacol* **2012,** *64*, 190-198.

7. Jeong, T. H.; Oh, S. G. Influence of the Ceramide(III) and cholesterol on the structure of a non-hydrous phospholipid-based lamellar liquid crystal : Structural and thermal transition behaviors. *Bull Kor Chem Soc* **2007,** *28*, 1021-1030.

8. Manconi, M.; Sinico, C.; Caddeo, C.; Vila, A. O.; Valenti, D.; Fadda, A. M. Penetration enhancer containing vesicles as carriers for dermal delivery of tretinoin. *Int. J. Pharm.* **2011,** *412*, 37-46.

9. Elmoslemany, R. M.; Abdallah, O. Y.; El-Khordagui, L. K.; Khalafallah, N. M. Propylene Glycol Liposomes as a Topical Delivery System for Miconazole Nitrate: Comparison with Conventional Liposomes. *AAPS PharmSciTech* **2012,** *13*, 723-731.

10. Wei-Ze, L.; Ning, Z.; Yong-Qiang, Z.; Li-Bin, Y.; Xiao-Ning, W.; Bao-Hua, H.; Peng, K.; Chun-Feng, Z. Post-expansile hydrogel foam aerosol of PG-liposomes: A novel delivery system for vaginal drug delivery applications. *Eur J Pharm Sci* **2012,** *47*, 162-169.

11. Jeong, T. H.; Oh, S. G. Lyotropic behaviors of a phospholipid-based lamella liquid crystalline phase hydrated by propylene glycol as a polar solvent: Correlation of DSPC vs PG concentration. *Bull Kor Chem Soc* **2007,** *28*, 108-114.

12. Pfeiffer, H. Hydration pressure and phase transitions of phospholipids. *Advances in Planar Lipid Bilayers and Liposomes* **2005,** *2*, 167-185.

13. Cunningham, B. A.; Bras, W.; Lis, L. J.; Quinn, P. J. Synchrotron X-ray studies of lipids and membranes: a critique. *J Biochem Biophys Meth* **1994,** *29*, 87-111.

14. Bigi, A.; Dovigo, L.; Koch, M. H. J.; Morocutti, M.; Ripamonti, A.; Roveri, N. Collagen structural organization in uncalcified and calcified human anterior longitudinal ligament. *Conn Tiss Res* **1991,** *25*, 171-179.

15. Evain, M.; Deniard, P.; Jouanneaux, A.; Brec, R. Potential of the Inel X-Ray Position-Sensitive Detector - a General Study of the Debye-Scherrer Setting. *J Appl Crystallogr* **1993,** *26*, 563-569.

16. Addink, E. J.; Beintema, J. Polymorphism of Crystalline Polypropylene. *Polymer* **1961,** *2*, 185-193.

17. Bliss, N.; Bordas, J.; Fell, B. D.; Harris, N. W.; Helsby, W. I.; Mant, G. R.; Smith, W.; Townsandrews, E. W16.1 - a New Fixed Wavelength Diffraction Station at the Srs Daresbury. *Rev Sci Instrum* **1995,** *66*, 1311-1313.

18. Quinn, P. J.; Wolf, C. Thermotropic and structural evaluation of the interaction of natural sphingomyelins with cholesterol. *Biochim Biophys Acta* **2009,** *1788*, 1877-1889.

19. Nagle, J. F.; Tristram-Nagle, S. Structure of lipid bilayers. *Biochim Biophys Acta* **2000,** *1469*, 159-195.

20. Blaurock, A. E.; Worthing.Cr. Treatment of low angle x-ray data from planar and concentric multilayered structures. *Biophys J* **1966,** *6*, 305-312.

21. McIntosh, T. J.; Magid, A. D.; Simon, S. A. Range of the solvation pressure between lipid membranes: dependence on the packing density of solvent molecules. *Biochem* **1989,** *28*, 7904-7912.

22. Quinn, P. J.; Takahashi, H.; Hatta, I. Characterization of complexes formed in fully hydrated dispersions of dipalmitoyl derivatives of phosphatidylcholine and diacylglycerol. *Biophys J* **1995,** *68*, 1374-1382.

23. Heenan, R. K.; Penfold, J.; King, S. M. SANS at pulsed neutron sources: present and future prospects. *J Appl Crystallogr* **1998,** *30*, 1140-1147.

24. Kotlarchyk, M.; Ritzau, S. M. Paracrystal model of the high-temperature lamellar phase of a ternary microemulsion system. *J Appl Crystallogr* **1991,** *24*, 753-758.

25. Shibayama, M.; Hashimoto, T. Small-angle x-ray scattering analyses of lamellar microdomains based on a model of one-dimensional paracrystal with uniaxial orientation. *Macromolecules* **1986,** *19*, 740-749.

26. Skipper, N. T.; Soper, A. K.; McConnell, J. D. C. The structure of interlayer water in vermiculite. *J Chem Phys* **1991,** *94*, 5751-5760.

27. Heenan, R. K. *FISH data analysis program*; 1989; 89–129.

28. Tristram-Nagle, S.; Zhang, R.; Suter, R. M.; Worthington, C. R.; Sun, W. J.; Nagle, J. F. Measurement of chain tilt angle in fully hydrated bilayers of gel phase lecithins. *Biophys J* **1993,** *64*, 1097-1109.

29. Li, S. J.; Kinoshita, K.; Furuike, S.; Yamazaki, M. Effects of solvents interacting favorably with hydrophilic segments of the membrane surface of phosphatidylcholine on their gel-phase membranes in water. *Biophys Chem* **1999,** *81*, 191-196.

30. Ueno, M.; Katoh, S.; Kobayashi, S.; Tomoyama, E.; Ohsawa, S.; Koyama, N.; Morita, Y. Evaluation of phase transition temperature of liposomes by using the tautomerism of □-benzoylacetoanilide. *J Coll Interf Sci* **1990,** *134*, 589-592.

31. Loomis, C. R.; Shipley, G. G.; Small, D. M. Phase-behaviour of hydrated cholesterol. *J Lip Res* **1979,** *20*, 525-535.

32. van Meer, G.; Voelker, D. R.; Feigenson, G. W. Membrane lipids: where they are and how they behave. *Nat Rev Mol Cell Biol* **2008,** *9*, 112-124.

33. ASTER, ASTER (Assessment Tools for the Evaluation of Risk) ecotoxicity profile. In ed.; U.S. Environmental Protection Agency, E. R. L., Ed. Duluth, MN, **1995**

34. Martino, A.; Kaler, E. W. The stability of lamellar phases in water, propylene-glycol, and surfactant mixtures. *Coll Surf A* **1995,** *99*, 91-99.

35. Ly, H. V.; Longo, M. L. Probing the interdigitated phase of a DPPC lipid bilayer by micropipette aspiration. *Macromol Symp* **2004,** *219*, 97-122.

36. Ly, H. V.; Longo, M. L. The influence of short-chain alcohols on interfacial tension, mechanical properties, area/molecule, and permeability of fluid lipid bilayers. *Biophys J* **2004,** *87*, 1013-1033.

37. Israelachvili, J. N., *Intermolecular and Surface Forces*. Second Edition ed.; Academic Press: London, 1991

38. Lee, C. H.; Lin, W. C.; Wang, J. P. All-optical measurements of the bending rigidity of lipid-vesicle membranes across structural phase transitions. *Phys Rev E* **2001,** *64,* 020901.

39. Scherfeld, D.; Kahya, N.; Schwille, P. Lipid dynamics and domain formation in model membranes composed of ternary mixtures of unsaturated and saturated phosphatidylcholines and cholesterol. *Biophys J* **2003,** *85*, 3758-3768.

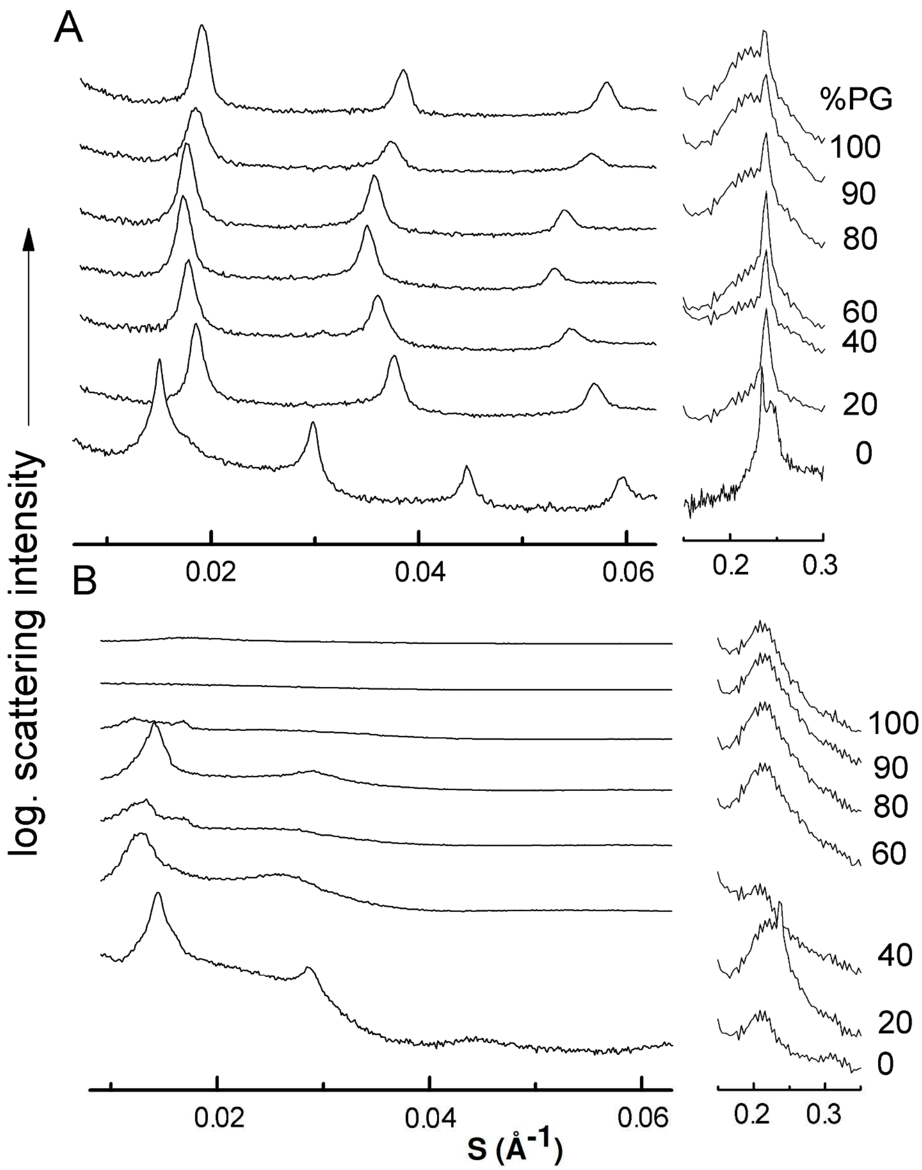

Figure 1. Small-angle (left) and wide-angle (right) X-ray scattering intensity profiles recorded from dispersions of distearoylphosphatidylcholine in various aqueous propylene glycol solutions (%PG w/w) at A. 25°C and B. 65°C.
731x902mm (96 x 96 DPI)

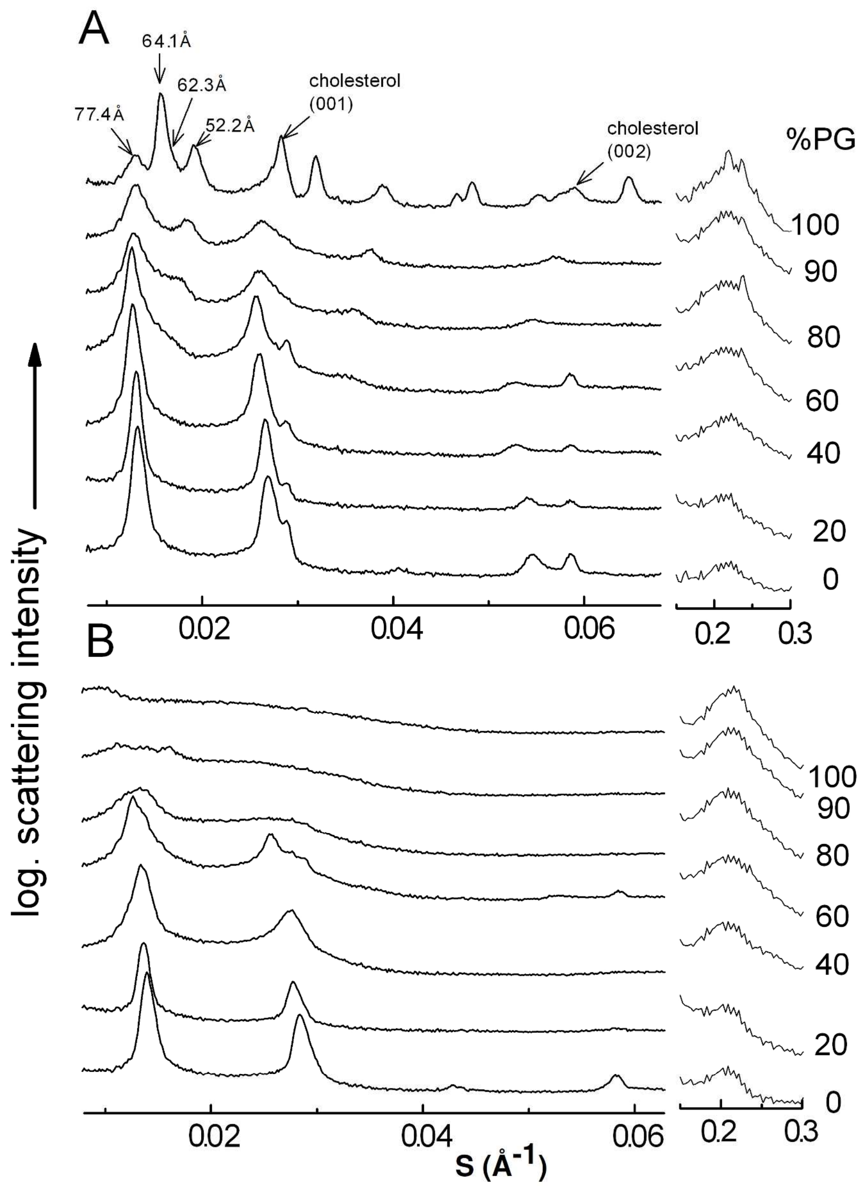

Figure 2. Small-angle (left) and wide-angle (right) X-ray scattering intensity profiles recorded from dispersions of equimolar mixtures of distearoylphosphatidylcholine and cholesterol in various aqueous propylene glycol solutions (%PG w/w) at A. 25°C and B. 65°C.
692x942mm (96 x 96 DPI)

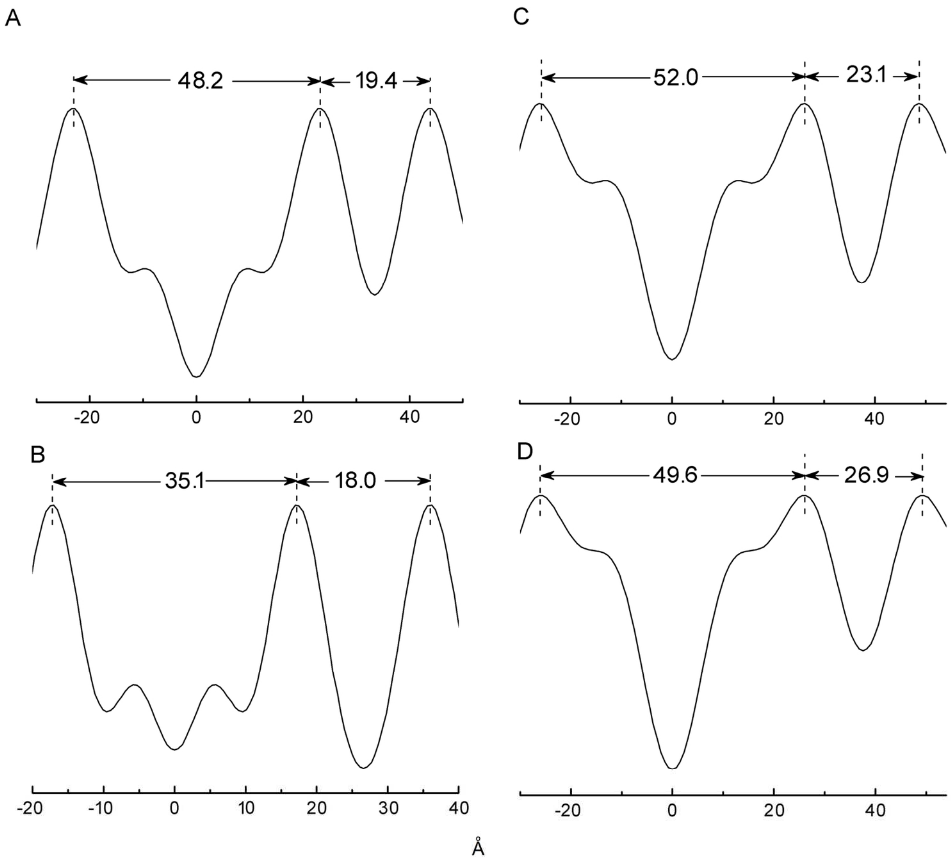

Figure 3. Representative electron density profiles calculated from small-angle X-ray scattering intensity profiles obtained at 25°C, of distearoylphosphatidylcholine dispersions in A. water and B. 20% w/w propylene glycol; dispersions of equimolar mixtures of distearoylphosphatidylcholine and cholesterol in C. water and D. 20% w/w propylene glycol.
143x125mm (300 x 300 DPI)

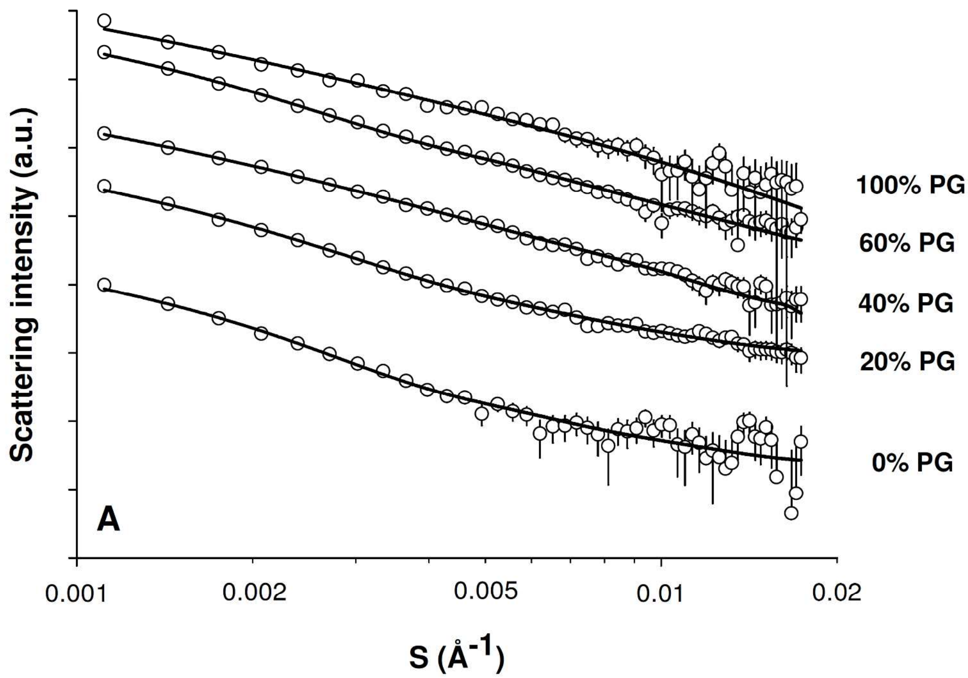

Figure 4. Small-angle neutron scattering intensity profiles recorded at 25°C from dispersions of A. d70-distearolyphosphatidylcholine in various hydrogenated aqueous solutions of propylene glycol (%PG w/w) and B. hydrogenated distearolyphosphatidylcholine in various deuterated aqueous solutions of propylene glycol (%PG w/w). The open circles show the experimental data and the solid lines show the fitted model. For some cases the error bars for these SANS scattering curves are very low and do not protrude beyond the symbols used to mark the points.
753x529mm (96 x 96 DPI)

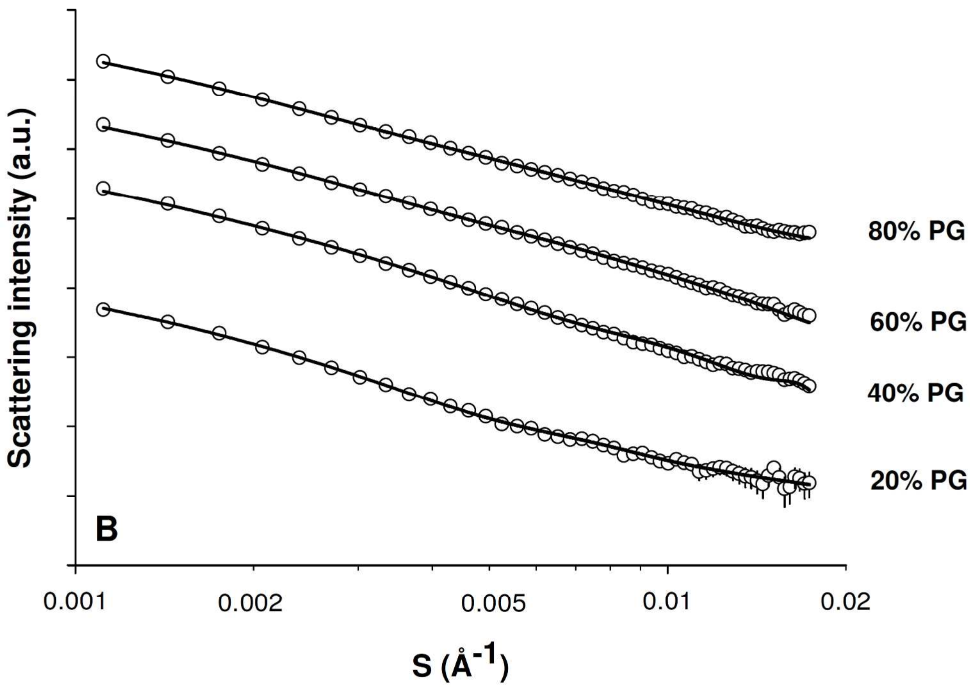

743x520mm (96 x 96 DPI)

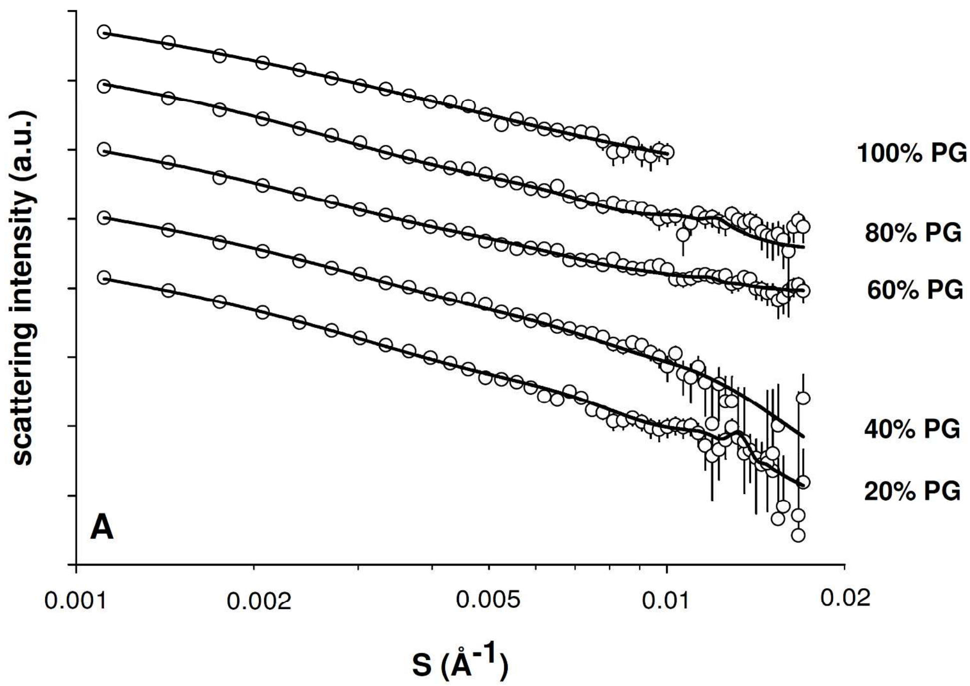

Figure 5. Small-angle neutron scattering intensity profiles recorded at 25°C from dispersions of equimolar mixtures of distearolyphosphatidylcholine and cholesterol containing A. d70-distearolyphosphatidylcholine in various hydrogenated aqueous solutions of propylene glycol (%PG w/w) and B. hydrogenated distearolyphosphatidylcholine in various deuterated aqueous solutions of propylene glycol (%PG w/w). The open circles show the experimental data and the solid lines show the fitted model. In some cases the error bars for these SANS scattering curves are very low and do not protrude beyond the symbols used to mark the points.
745x522mm (96 x 96 DPI)

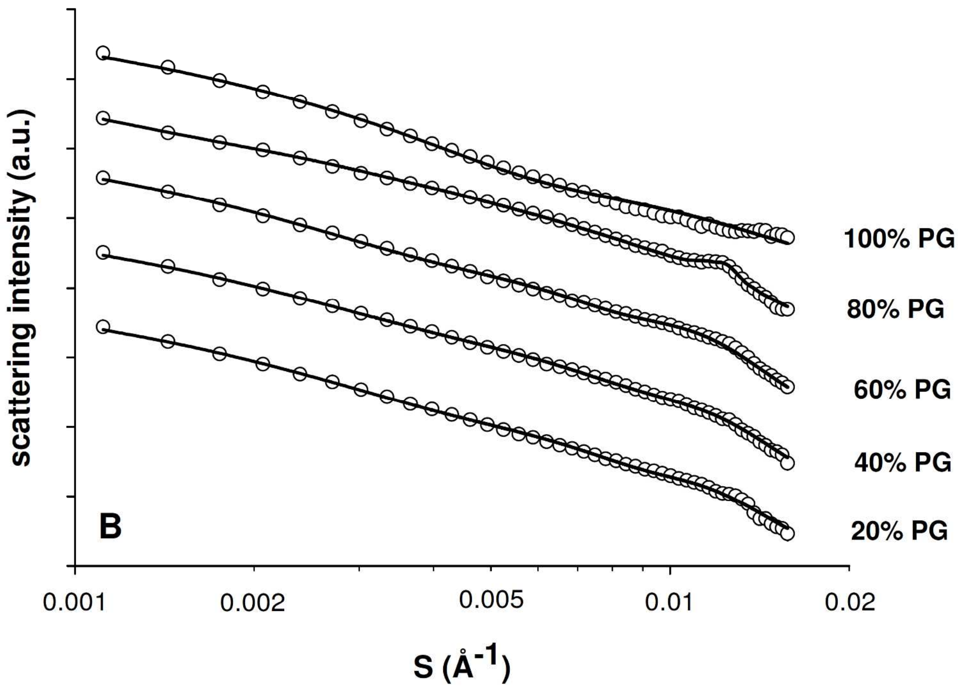

739x522mm (96 x 96 DPI)

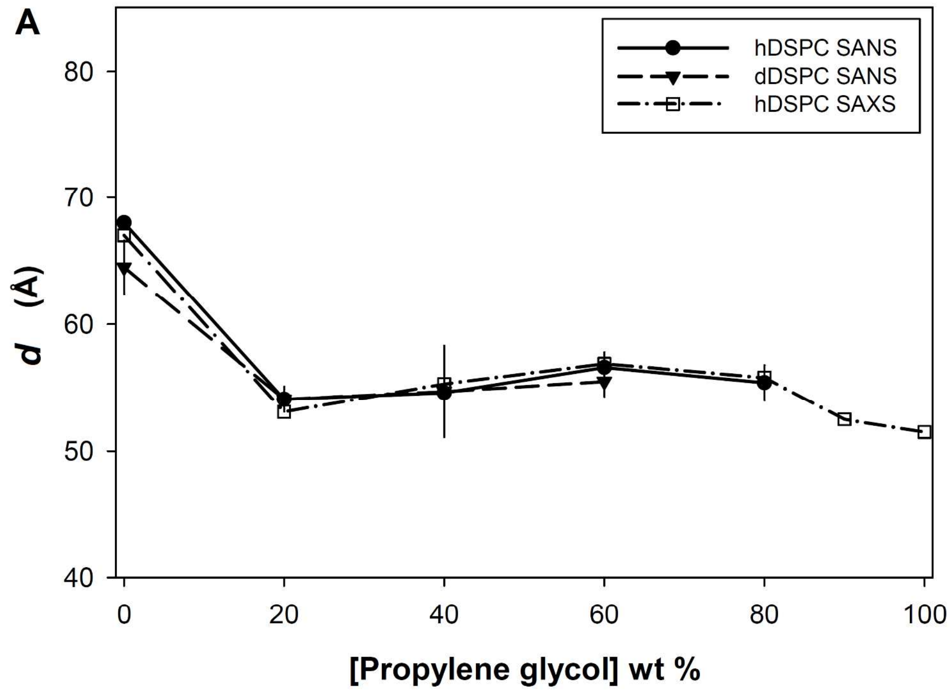

Figure 6. Summaries of bilayer parameters obtained from measurements of DSPC (A,C & E) and DSPC/cholesterol (B, D & F) dispersions in propylene glycol solutions using both small-angle X-ray and small-angle neutron scattering techniques: A and B represent the lamellar repeat spacings (d), C and D represent the bilayer thicknesses (dm) and E and F represent the solvent layer thicknesses (ds).
712x515mm (96 x 96 DPI)

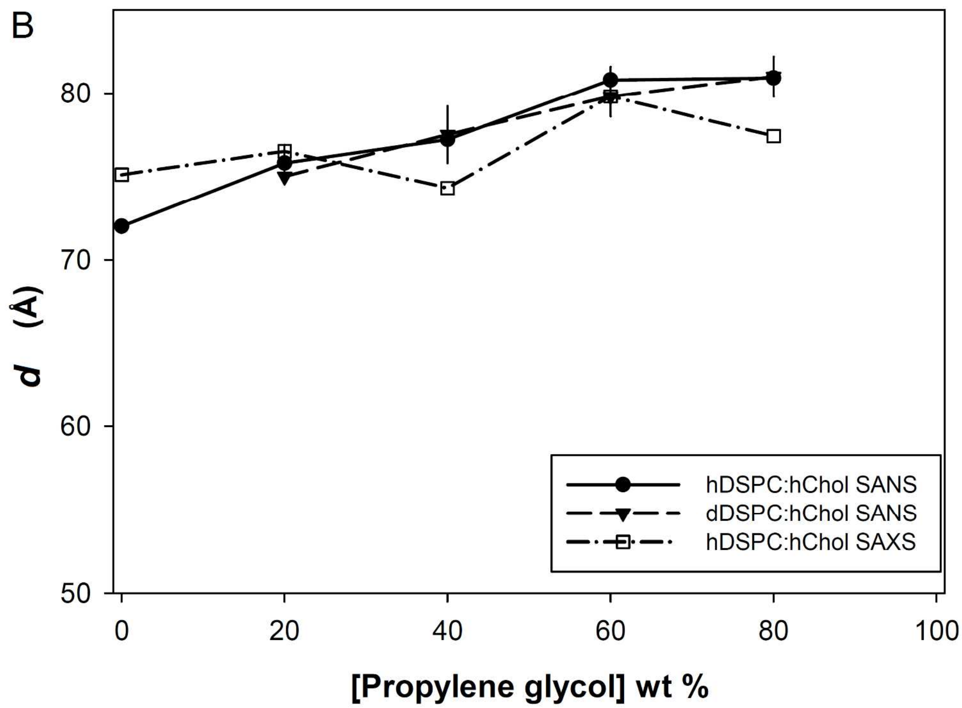

699x510mm (96 x 96 DPI)

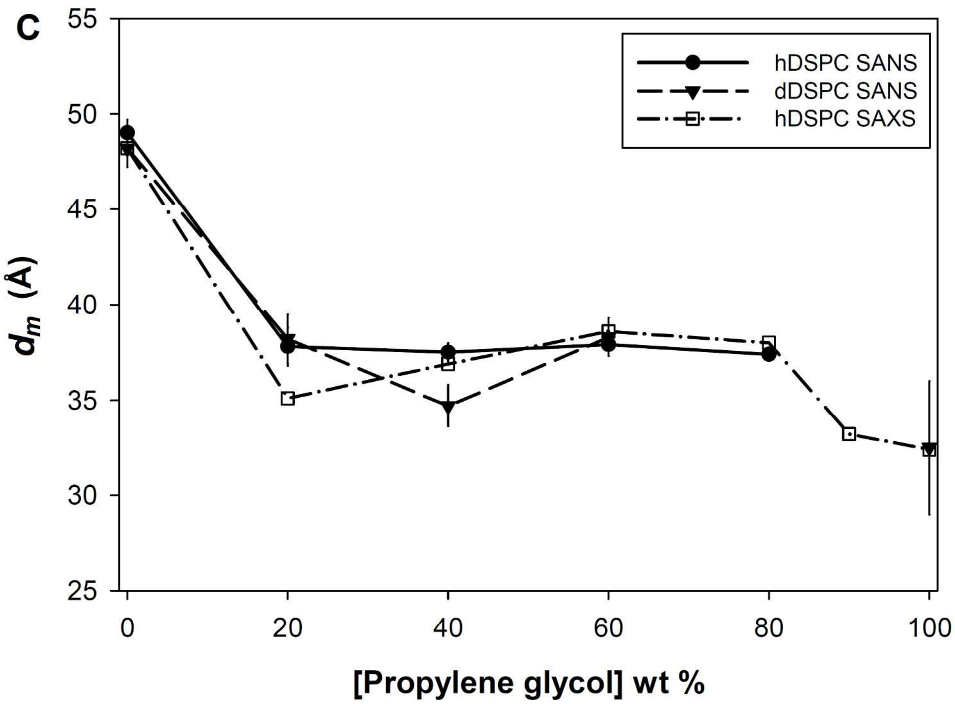

711x522mm (96 x 96 DPI)

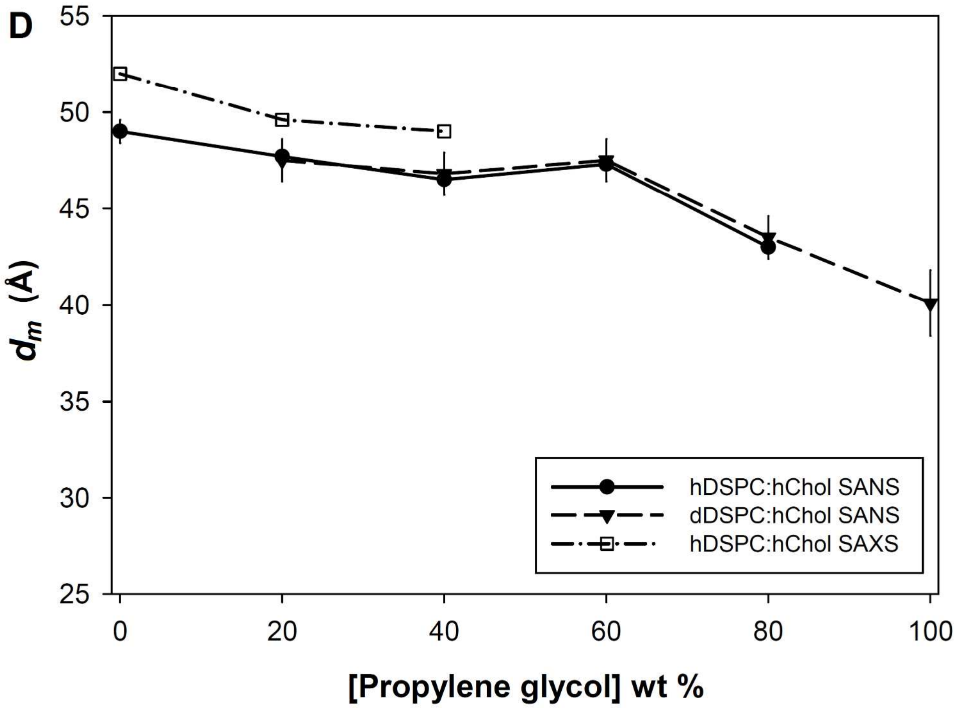

704x520mm (96 x 96 DPI)

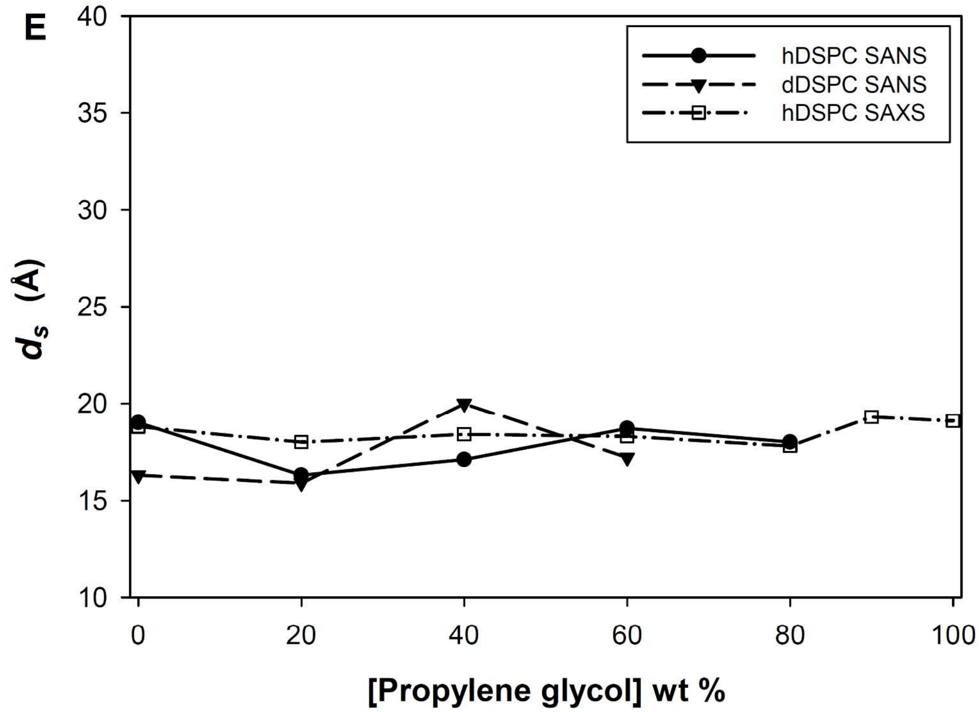

700x518mm (96 x 96 DPI)

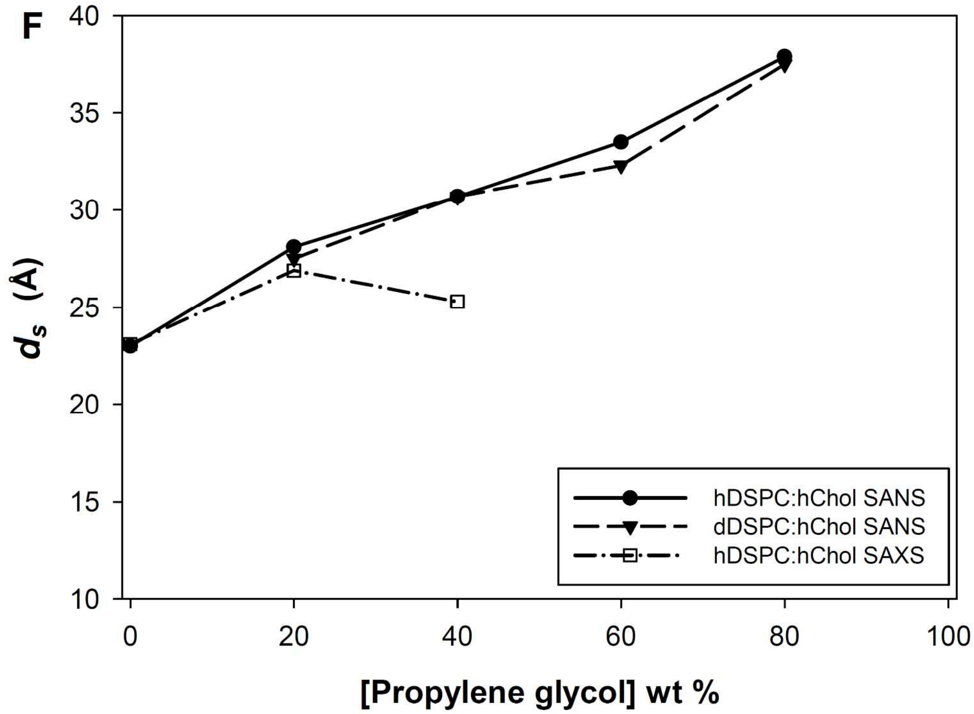

697x514mm (96 x 96 DPI)

Figure 7. Freeze-fracture electron micrographs of dispersions of equimolar mixtures of distearoylphosphatidylcholine and cholesterol in A. 20% w/w propylene glycol, B. 60% w/w propylene glycol and C. 100% w/w propylene glycol. In micrograph A, the arrow indicates the appearance of a lamellar stack. In each micrograph, the scale bar represents 200 nm.
69x48mm (300 x 300 DPI)

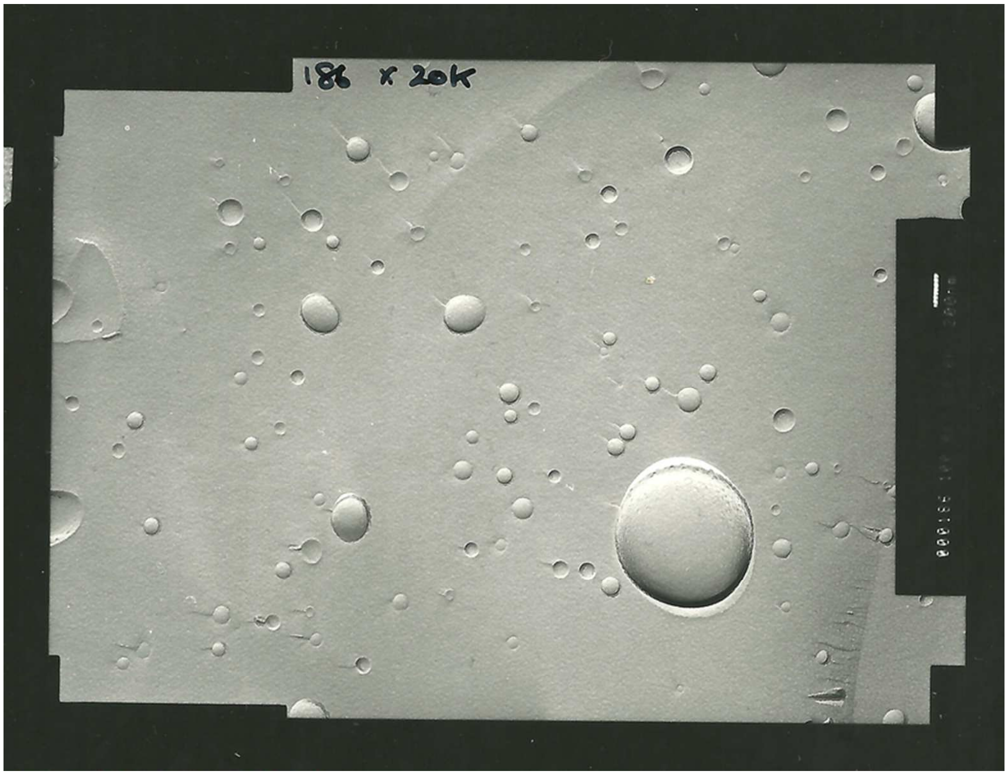

73x56mm (300 x 300 DPI)

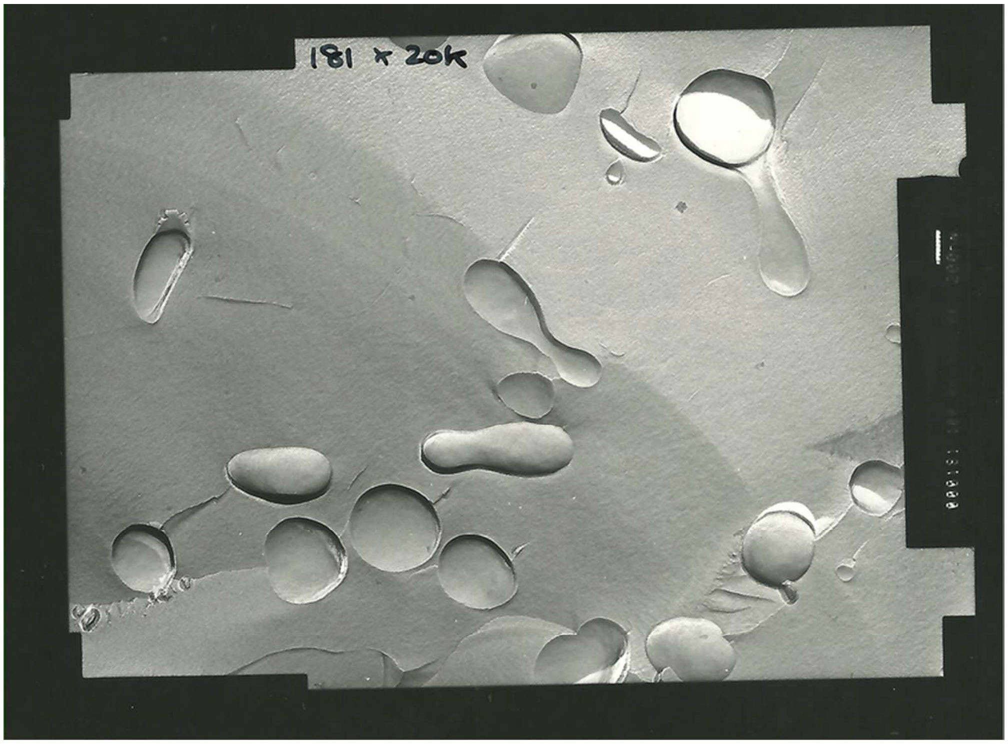

71x52mm (300 x 300 DPI)

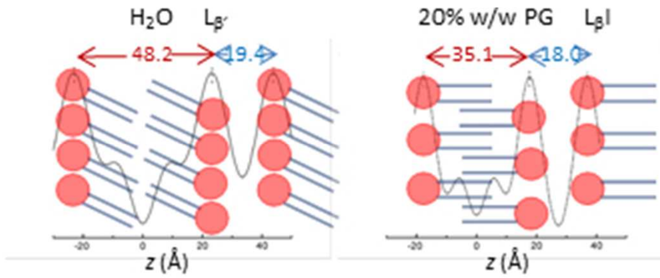

88x35mm (96 x 96 DPI)